journal

J. Am. Ceram. Soc., 78 [1] 49–57 (1995)

Powder Processing for the Fabrication of Si_3N_4 Ceramics: I, Influence of Spray-Dried Granule Strength on Pore Size Distribution in Green Compacts

Hidehiro Kamiya,*,† Kenji Isomura, and Genji Jimbo

Department of Chemical Engineering, Nagoya University, Nagoya 464-01, Japan

Tsubaki Jun-ichiro

Japan Fine Ceramics Center, Nagoya, Japan

The effect of spray-dried granule strength on the microstructure of green compacts obtained by isostatic pressing was quantitatively analyzed. The fracture strength of single granules of Si_3N_4 powder made with ultrafine Al_2O_3 and Y_2O_3 powders was measured directly by diametral compression. It was found that fracture strength increased notably with the increasing relative density of the granule and the decreasing size of agglomerates in suspension before spray-drying. Even when green bodies were prepared at an isostatic pressure of 200 MPa, intergranular pores, which negatively affected densification of the sintered bodies, occurred between unfractured granules. The volume and size of these pores in the green compacts increased with the increasing fracture strength of the granules. In the case of closely packed granules, an isostatic pressure of 800 MPa was required to completely collapse the intergranular pores. A simple equation was derived to calculate the isostatic pressure necessary for complete collapse of intergranular pores in the green compacts, and it was determined that granule strength must be kept as low as possible to obtain uniform green compacts.

I. Introduction

Powders smaller than 1 μm in diameter hold promise as raw materials for the fabrication of advanced ceramics. The strong and open agglomeration of these fine powders, however, deters the close and uniform packing of the resulting compacts. The effects of granule strength,[1] adsorbed moisture[1,2] in the granule, and the concentration of an admixed organic plasticizer[3]/binder[1–7] on green density and the pressure–density curve have been investigated for the dry pressing of spray-dried granules. In those studies, compacts pressed from softer granules exhibited higher density, with more complete joining, and higher strength after drying. In addition, the binder acted as a lubricant, assisting particle sliding at a higher formation pressure. Few researchers, however, have investigated the effect of agglomeration in the powder suspension[7] on the microstructures of the green compact and the granule before spray drying. Slip casting and colloidal forming techniques[8–20] have focused more attention on agglomeration in suspension, and the interrelationships between powder characteristics and green compact microstructure and sintering behavior have been discussed. Uematsu *et al.*[21,22] observed intergranular pores between unfractured spray-dried granules by a liquid immersion technique, even in green bodies prepared at 600 MPa. Adjusting the strength and microstructure of spray-dried granules thus becomes an important issue for achieving high reliability and high strength in ceramics. Furthermore, the effects of agglomeration in suspension on the green compact and the spray-dried granular microstructure of non-oxide ceramics[23–25] have not been systematically evaluated.

For the present study, the size of the agglomerates in suspension and the strength and microstructure of the spray-dried granules of Si_3N_4 powders were varied by changing the amounts of organic dispersants. The fracture strength of a single granule was measured directly by diametral compression. The microstructures of the granules and the green compacts were investigated by mercury porosimetry. Correlations between the strength of the granules and the green microstructure (both inter- and intragranular pores) were analyzed quantitatively, and the optimum powder-processing conditions for obtaining uniform green compacts of Si_3N_4 powders with small and narrow porosity are discussed in this paper.

II. Experimental Procedure

(1) *Preparation of Spray-Dried Granules*

Fine powders of Si_3N_4 produced by the thermal decomposition of silicon imide (SN-E10, Ube Industries, Yamaguchi, Japan) were mixed and dispersed in water with 3 and 5 wt% ultrafine γ-Al_2O_3 and Y_2O_3 powders by ball milling for 96 h. The properties of the powders are shown in Table I. Ultrafine powders of Al_2O_3 and Y_2O_3 have larger specific areas than does Si_3N_4 powder. The size distributions of the powder agglomerates in suspension were varied by changing the amounts of maleic anhydride polymer (AKM0531, Nippon Oil and Fats, Tokyo, Japan) used as a water-soluble dispersant (concentration (C_D) = 0, 1, 2, and 4 wt%). The samples then were characterized by light scattering and diffraction (Cilas Granulometer HR850, Cilas, France). Figure 1 shows the structure of the maleic anhydride polymer. When the molecular weight of this polymer is less than 20 000 to ~30 000 ($k < 100$), the chain cross-links with other molecules during the heating phase of spray drying, and the polymer behaves as a binder within the spray-dried granules. The properties of the polymer as a binder were hindered in the present work, however, by its long-chain structure ($k > 1000$).

The viscosity of each suspension was determined with a concentric cylinder viscometer at a shear rate of 1 s^{-1}. After the powders had been mixed for 96 h, they were spray dried (CL-8, Ohkawara Kakohki, Yokohama, Japan) at 170°C. In the samples with no dispersants (C_D = 0 wt%), water (about

J. W. Halloran—contributing editor

Manuscript No. 194486. Received June 9, 1993; approved August 22, 1994.
*Member, American Ceramic Society.
†Now with Department of Chemical Engineering, Tokyo University of Agriculture and Technology, Koganei, Tokyo 184, Japan.

Table I. Powder Properties of Raw Materials

Raw material	Si_3N_4	Al_2O_3	Y_2O_3
True density, ρ_I (g/cm^3)	3.20	3.67	5.03
ζ-potential, pH ~7 (mV)	−19.3	11.0	21.2
Sw (m^2/g)	11.0	151	24.8
d_B (nm)	170	10.8	48.1

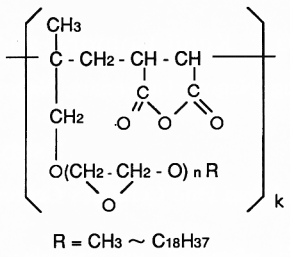

Fig. 1. Schematic of maleic anhydride polymer segment.

0.0006 m^3/0.00/m^3 suspension) was added to decrease the viscosity of the suspension before spray drying.

(2) Characterization of the Granules

The tensile strength (σ_T) of a single granule was measured using a commercial testing machine (MCTE-200, Shimadzu, Kyoto, Japan). Each single, spherical granule was tested between parallel platens with polished surfaces and crushed alone in diametral compression at a loading rate of 0.01 g/min. The specimen then was put on the polished plate of an ultrahard metal and uniaxially compressed by the circular plate of a diamond 50 μm in diameter. The relationship between load and displacement during loading was determined. The size distribution of the granules was characterized by light scattering and diffraction (Cilas Granulometer) and by image processing through a scanning electron microscope. The measurements by the two methods were in near agreement. The microstructures of the granules were observed by scanning electron microscopy (SEM). The pore size distribution and porosity ratio of the granules were measured by mercury porosimetry (Poresizer 9310, Micromeritics, Norcross, GA). The size distribution of the granules was characterized by light scattering without ultrasonic dispersion.

(3) Preparation and Characterization of Green Compact

The granules were packed into a cylindrical cell 2 cm in diameter and uniaxially pressed at 10 MPa for 3 min. The compacts then were consolidated by cold isostatic pressing in the range from 20 to 800 MPa (MCT-100, Mitsubishi Heavy Industries, Tokyo, Japan). The green density was determined from the specimen weight and dimensions. The compact pore size distribution was measured by mercury porosimetry.

III. Results

(1) Characterization of Suspension

The viscosities of the suspensions after 96 h of mixing are shown in Table II. The minimum viscosity of the suspensions occurred at a dispersant concentration, C_D, of 2 wt% for a sintering aid concentration, C_A, of 5 wt%, and at C_D = 1 wt% for C_A = 3 wt%. The size distributions of the powder agglomerates in suspension are shown in Fig. 2. The minimum mean diameter of the agglomerates was exhibited at C_D = 2 wt% for C_A = 5 wt% and at C_D = 1 wt% for C_A = 3 wt%. The minimum viscosity and size of agglomerates in suspension appeared at the same dispersant concentration. Excess dispersant increased the viscosity and promoted powder agglomeration. The minimum agglomerate viscosity and size were achieved when the amount of dispersant was increased with an increasing concentration of the ultrafine sintering aids. The large surface area of the ultrafine powders caused most of the dispersant to be adsorbed onto the surfaces of the sintering aids.

(2) Structure and Strength of Spray-Dried Granules

The size distribution of the spray-dried granules was similar in all cases (Fig. 3). The mean diameter of the granules was about 45 μm. The pore size distributions in packed beds of granules before uniaxial or isostatic pressing are shown in Figs. 4(A) and (B). A bimodal pore size distribution was

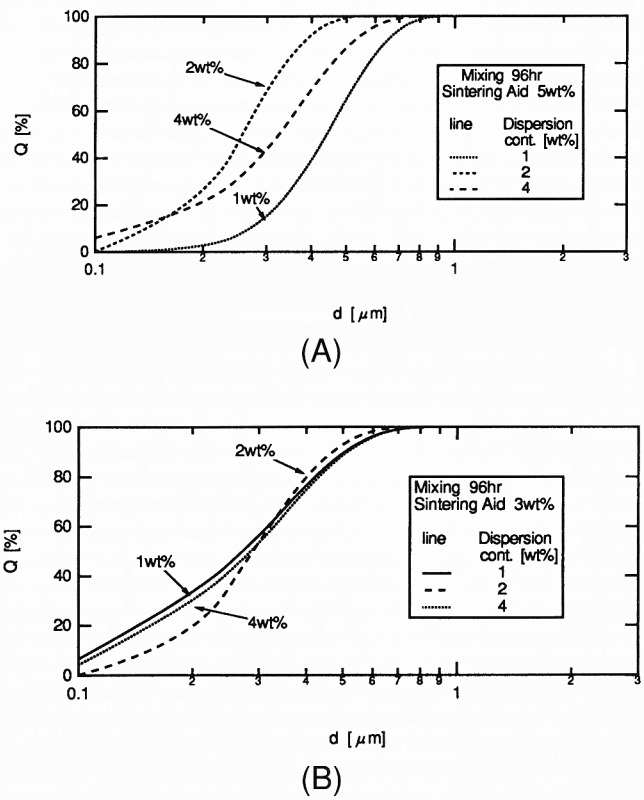

Fig. 2. Size distribution for agglomerates in suspension after 96 h milling. Concentration of sintering additives (C_A, ultrafine Al_2O_3 and Y_2O_3 powders) were (A) 5 wt% and (B) 3 wt%.

Table II. Properties of Suspension after 96 h Mixing

C_A (wt%)	Al_2O_3 = 5, Y_2O_3 = 5				Al_2O_3 = 3, Y_2O_3 = 3		
C_D (wt%)	0	1	2	4	1	2	3
Viscosity (cp)*	329	18.6	17.8	35.3	19.5	33.4	41.7
Sw (m^2/g)	16.3	19.0	26.2	26.3	21.7	22.3	23.6

*cp = 10^{-3} Pa·s.

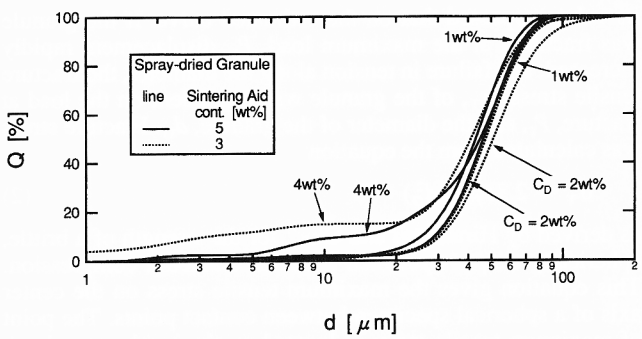

Fig. 3. Size distribution for spray-dried granules.

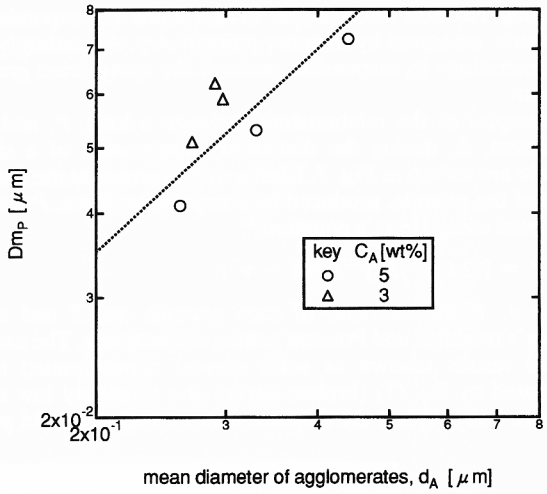

Fig. 5. Relations between mean diameter (d_A) of agglomerates in suspension and peak of interparticle pore diameter (Dm_P) in spray-dried granules.

observed in all cases. The peak at a large pore diameter corresponded to intergranular pores (Dm_G) and that at a small pore diameter to interparticle (Dm_P) pores. The peak diameter and volume of the intergranular pores were similar in all cases. The minimum interparticle mode pore diameter occurred at C_D = 2 wt% for C_A = 5 wt% and at C_D = 1 wt% for C_A = 3 wt%. The minimum mean diameter of the agglomerates in suspension occurred at the same concentration of dispersants (Fig. 2), and the dependence of the amount of dispersant on the interparticle mode pore diameter and size distribution of the agglomerates (Fig. 2) decreased with decreasing amounts of sintering aids. The relationship between the peak of intragranular pore diameter (Dm_P) and the mean diameter (d_A) of the powder agglomerates in suspension is shown in Fig. 5. The peak of the intragranular pore diameter (Dm_P) increased in proportion to the mean diameter (d_A) of the powder agglomerates in suspension. Some examples of spray-dried granules are shown in Fig. 6. A rough surface and porous structure were observed in the granules at C_D = 0 wt%, shown in Fig. 6(A), because of powder agglomeration in the suspension. For C_D = 2 wt%, shown in Fig. 6(B), the primary particles were closely packed in the granules by the capillary force created during spray drying.

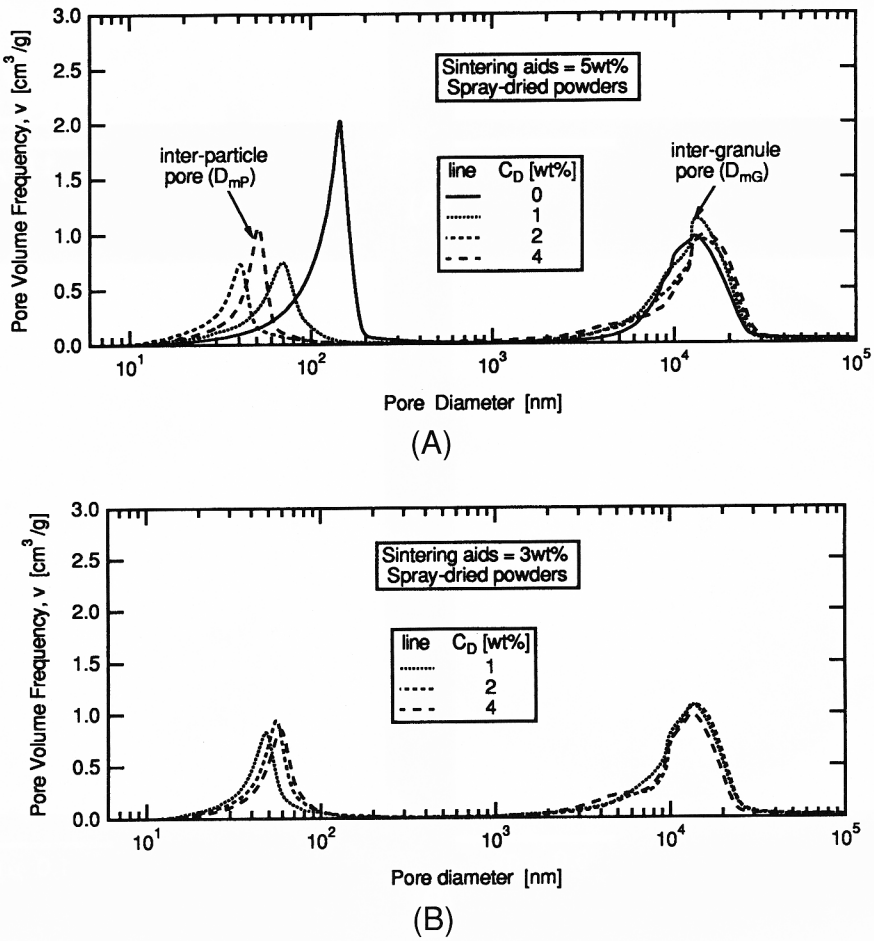

Fig. 4. Pore size distribution in packed beds of spray-dried granules before pressing. Concentration of sintered additives (C_A) were (A) 5 wt% and (B) 3 wt%.

Scanning electron microscopic observations corresponded to the results measured by mercury porosimetry. Accordingly, the agglomerations in suspension retained the spray-dried granule structure.

Examples of the relationships between a load, P, and displacement, Δ, during the diametral compression of a single granule are shown in Fig. 7. Elastic displacement at the contact point of the granule, produced by compressive force, P, can be estimated using Hertz's equation,[19]

$$P = [(2d_G Y^2)\Delta^3]^{1/2}/[3(1 - \nu^2)] \quad (1)$$

where d_G is the diameter of each granule, and Y and ν are Young's modulus and Poisson's ratio, respectively. The experimental results (shown as solid curves) approximated those calculated by Eq. (1) (broken curve) at a relatively low compressive force. When the displacement exceeded a yield point, its value surpassed that on the estimated curve. If the granule was fractured at the maximum load, P_f, displacement rapidly increased. For failure in tension along the diameter, the fracture tensile stress, σ_T, of the granule was dependent on the load at fracture, P_f, and the diameter of the granule, d_G. Fracture stress was calculated from the equation

$$\sigma_T = 2.8P_f/(\pi d_G^2) \quad (2)$$

as derived by Hiramatsu and Oka[27] for the strength of a brittle, spherically shaped specimen tested in diametral compression. This equation gives the maximum tensile stress on the center axis of a spherical specimen between contact points. The point of maximum tensile stress is located on the inside, at a depth equal to about one-half the radius of the contact surface. Accordingly, if local plastic deformation occurred at a contact point and one-half the width of the contact surface increased to

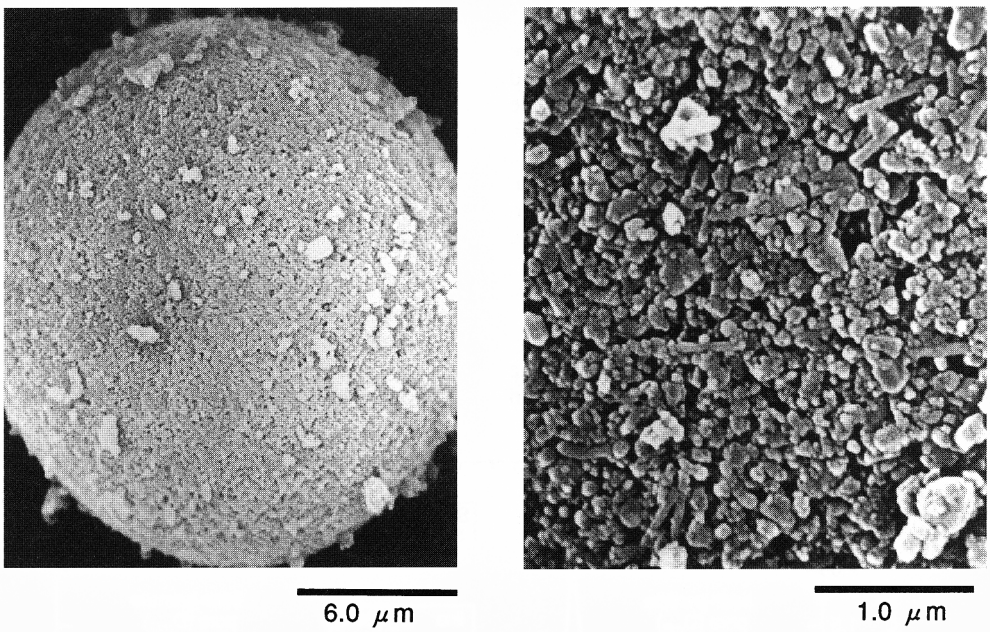

Fig. 6. SEM observations for spray-dried granules (C_A = 5 wt%). Concentrations of water-soluble maleic anhydride dispersant were (A) 0 wt% and (B) 2 wt%.

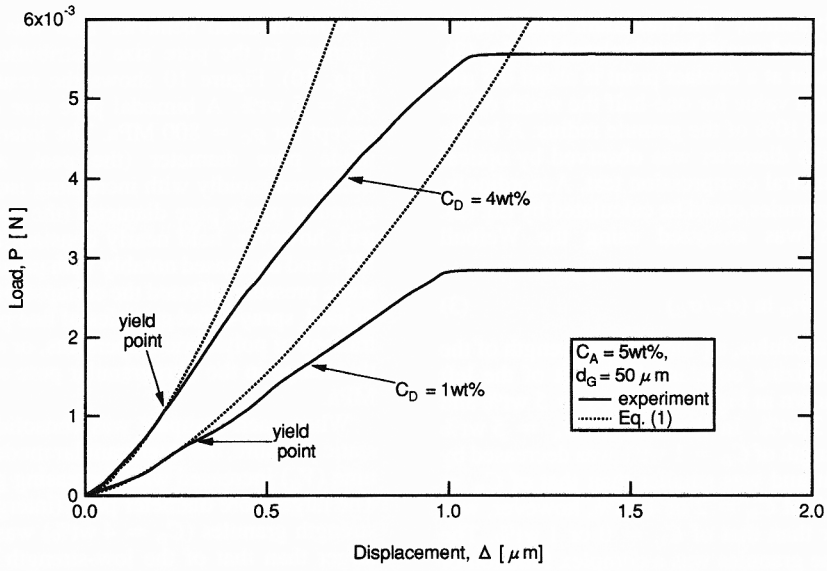

Fig. 7. Examples of relation between loading force and displacement during diametral compression for a single granule.

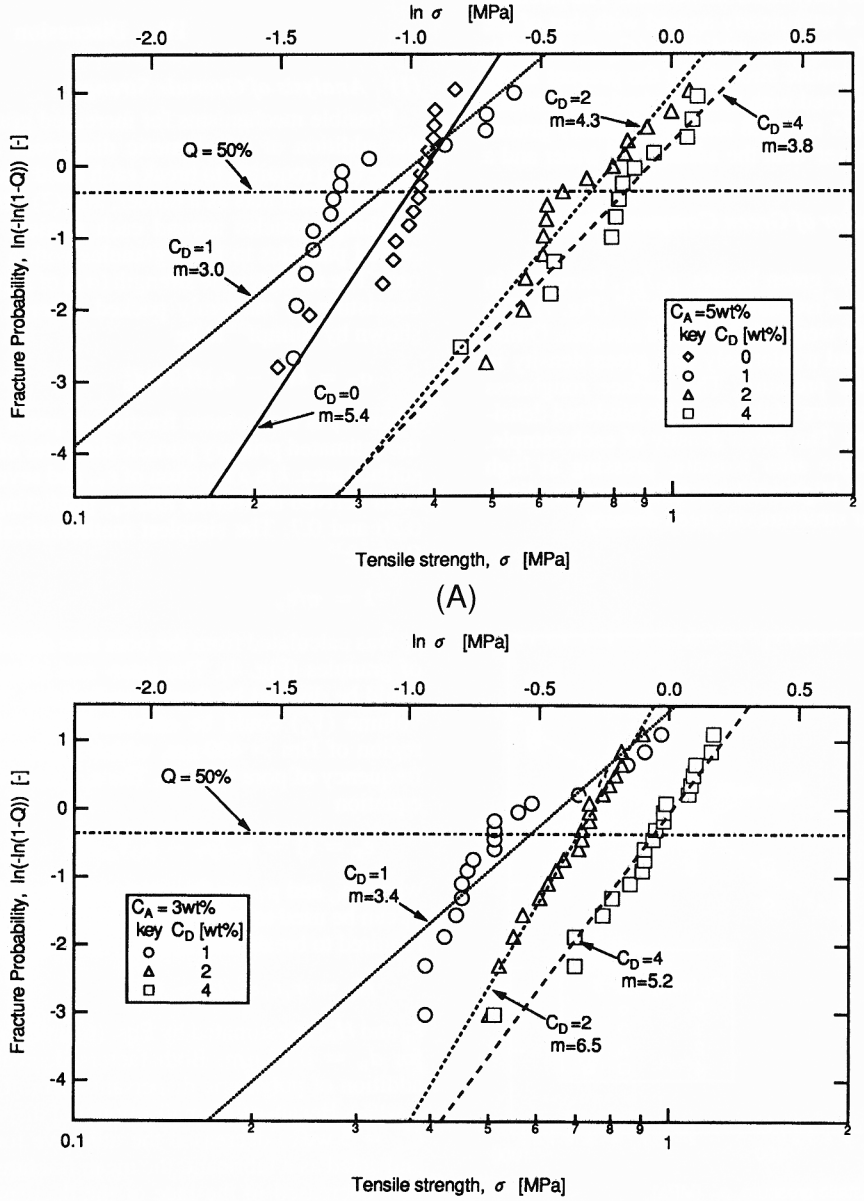

Fig. 8. Distributions of tensile fracture strength for spray-dried granules. Concentrations of sintered additives (C_A) were (A) 5 wt% and (B) 3 wt%.

10% of the spherical body radius,[20] the maximum tensile stress would be nearly constant and could be calculated by Eq. (2). The maximum displacement at a contact point is about 0.5 μm in Fig. 7, and the calculated value for one-half the width of the contact surface is less than 10% of the granule radius. A brittle failure in tension along the diameter was observed by optical microscopy after the diametral compression test. Accordingly, the fracture stress of the granules could be calculated by Eq. (2).

The fracture strength was analyzed using the Weibull distribution,

$$\ln \ln [1/(1 - Q)] = m_G \ln (\sigma_T/\sigma_C) \quad (3)$$

where m_G is the Weibull modulus, σ_T the tensile strength of the granules, and σ_C a normalizing constant. The plot of the left side of Eq. (3) vs σ_T is shown in Fig. 8(A) for C_A = 5 wt% and in Fig. 8(B) for C_A = 3 wt%. In the case of C_A = 5 wt% (Fig. 8(A)), the mean strength of C_D = 1 wt% was decreased by the addition of dispersant and was smaller than that of C_D = 0 wt%. The mean strength of C_D = 2 or 4 wt%, however, was two or three times larger than that of C_D = 0 or 1 wt%. The strength distribution of the granules was a complex function of the amount of polymeric dispersants. In the case of C_A = 3 wt% (Fig. 8(B)), the mean strength of the granules increased with increasing amounts of polymeric dispersant. The strength distribution of C_D = 2 or 4 wt% nearly agreed with that of the different concentration of sintering additives (C_A = 5 wt%). The Weibull modulus of granule strength in the present study (m_G = 3 to ~6.5) nearly agreed with that of spherical aluminosilicate agglomerates[21] (0.95 to ~1.8 mm in diameter) granulated in a high-intensity mixer with the addition of water and a starch binder.

(3) Consolidation Behavior of Green Compacts under Isostatic Pressing

The relative density of the green bodies, ρ_G/ρ_T, increased in proportion to the logarithm of isostatic pressure[22,23] (Fig. 9). The slopes of these relationships were similar for all samples. Omission of the dispersant caused a relatively low green density in the region of low isostatic pressure. The surface roughness (Fig. 6(A)) and porous structure of the granules hindered densification of the green bodies. The green density of each sample, however, remained the same after isostatic pressing at high pressure (p_C = 800 MPa). High cold isostatic pressure eliminated the effect of granular structure on green density.

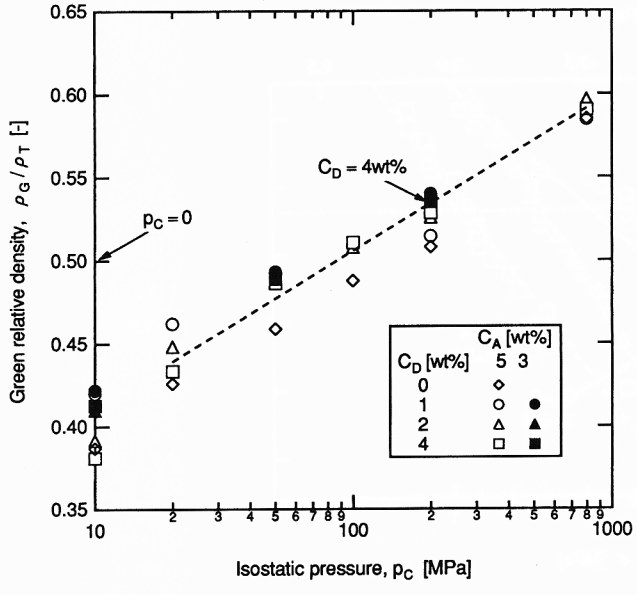

Fig. 9. Relations between green relative density and isostatic pressure.

Consolidation behavior also was examined, by measuring changes in the pore size distribution after isostatic pressing (Fig. 10). Figure 10 shows the results for C_D = 2 wt% and C_A = 5 wt%. A bimodal pore size distribution was observed except for p_C = 800 MPa. The intergranular pore volume and mode pore diameter (the peak at larger pore diameter) decreased rapidly with increasing isostatic pressure. The intragranular mode pore diameter (the peak at smaller pore diameter), however, held nearly constant in the range of $p_C < 200$ MPa and decreased notably with pressing at 800 MPa. High isostatic pressure affected the collapse of the agglomerate structure in hard, spray-dried granules of fine powders.[24,25] Other concentrations of polymeric dispersants, or sintering aids, revealed little change in the intragranular pore size in the range $p_C \leq 200$ MPa.

When each compact was consolidated under the same isostatic pressure, the intergranular mode pore size (Dm_G) and volume (V_G) increased with increasing granule strength (Fig. 11). The larger pore diameter peak (intergranular pore) of the high-strength granules (C_D = 4 wt%) was about 500 nm, 2.5 times larger than that of the low-strength granules (C_D = 1 wt%). Pore size distribution in the green compacts depended on the strength of the granules.

IV. Discussion

(1) Analysis of Granule Strength

Possible mechanisms for increased granule strength through the addition of a polymeric dispersant are (1) the increased force (H_P) required to break each bond between particles, where the dispersant acts as a binder, and (2) the increased number of touching particles around each particle (k), causing the dispersed particles to form granules with a closely packed structure. The mean tensile strength (σ_T) of a granule or a green body consisting of randomly packed spheres of uniform size was shown by Rumpf[33] to be

$$\sigma_T = k(1 - \varepsilon_P)H_P/\pi d_B^2 \quad (4)$$

where ε_P is the volume fraction of pores in the granule and d_B the estimated primary particle diameter of Si_3N_4 from a specific surface area. k is a function of ε_P, and several relationships have been derived between k and ε_P, predicting an ε_P value between 0.26 and 0.7. The simplest mathematical relation is given by Rumpf:[33]

$$k = \pi/\varepsilon_P \quad (5)$$

ε_P was calculated from the pore size distribution in packed beds of granules (Fig. 4). The inter- and intragranular pore volume could be divided by these distributions. The intergranular pore volume (V_G) could be calculated by the total volume in the region of Dm > 400 nm, which appeared to be the minimum frequency of pore volume. The ε_P values were estimated by the equation

$$\varepsilon_P = (1 - \rho_G/\rho_T - \rho_G V_G)/(1 - \rho_G V_G) \quad (6)$$

where ρ_G and ρ_T are the green density and true powder density. ε_P can be used to calculate, from Eqs. (4) and (5), the force (H_P) required to break each bond between primary particles. Thus,

$$H_P = \sigma_T \varepsilon_P d_B^2/(1 - \varepsilon_P) \quad (7)$$

ε_P and H_P, as estimated by Eqs. (6) and (7), are shown in Fig. 12 for d_B = 0.17 μm. Both factors decreased notably with the addition of polymeric dispersants (from C_D = 0 wt% to C_D = 1 wt%). Because the small amount of dispersants (C_D = 1 wt%, C_A = 5 wt%) decreased the adhesive force between particles and acted as a lubricant, the mean fracture strength of the granules decreased in the face of the decreased granular porosity. For C_D = 2 wt%, the estimated adhesive force had nearly the same value, with C_D = 0 wt%. The mechanisms for increasing granular strength can be explained by the increased number of

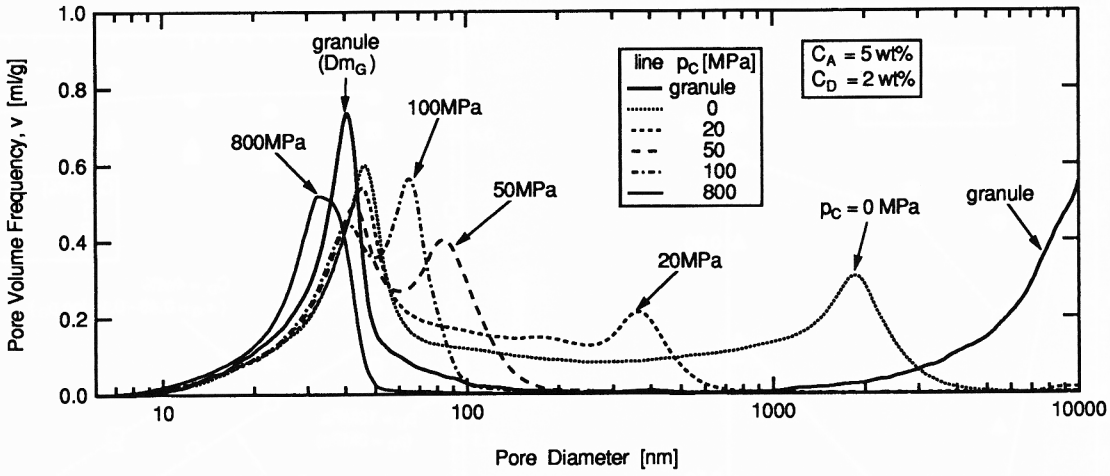

Fig. 10. Change of pore size distributions in green compacts after isostatic pressing. Concentration of sintering additives (C_A) was 5 wt% and polymeric dispersant (C_D) was 2 wt%.

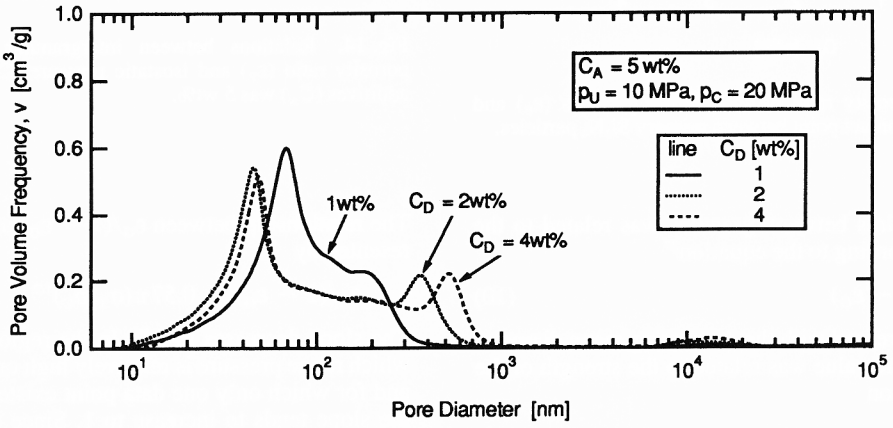

Fig. 11. Effects of concentration of dispersants and/or tensile strength of granule on the pore size distribution in compacts after isostatic pressing at 20 MPa.

touching particles around each particle (k). The closely packed structure of the granules, resulting from the fine dispersion of the agglomeration in suspension, caused the increase in granular strength.

The excess addition (from C_D = 4 wt%) of dispersants, however, increased both H_P and ε_P. The excess addition of dispersants caused the chain to cross-link with other molecules during the heating phase of spray drying, and the polymer then behaved as a binder within the spray-dried granules. The mean diameter of the agglomerates in suspension increased with the excess dispersants (from C_D = 2 wt% to C_D = 4 wt%, in Fig. 2). This fact suggests that a looser packing structure is formed in the granules by an agglomeration in suspension. The main mechanism for increasing granular strength in the face of increasing granular porosity is the notable increase of adhesive force at the contact points between particles because of excess dispersants. The complex dependence of the amount of dispersant on granular strength can be explained by changes in the adhesive force between particles and the packing structure in the granules.

(2) Effect of Strength on Green Microstructure

The pore size distribution in green compacts depends on the strength of the granules (Fig. 11). Relationships between green body microstructure and granular strength are analyzed quantitatively in the present study. The interparticle pore size distribution can be fitted by Gauss's equation (Fig. 13).

$$v = k_1 \exp[(D - \mathrm{Dm_P})^2/k_2] \quad (8)$$

Here, k_1 and k_2 relate the height of the peak and the width of distribution, respectively. The remaining intergranular volume (V_G) in the compacts corresponds to the total volume outside the fitted curve. The intragranular porosity (ε_P) is calculated from Eq. (6), and the intergranular porosity (ε_G) from the following equation:

$$\varepsilon_G = \rho_G V_G \quad (9)$$

The intergranular porosity (ε_G) of each sample decreased in proportion to the logarithm of isostatic pressure, but the intragranular porosity (ε_P) held nearly constant in the region $p_C <$ 800 MPa (Fig. 14). The intergranular porosity of C_D = 1 wt% was smaller than that of C_D = 2 or 4 wt%, and complete collapse may have occurred at 300 to ~400 MPa. On the other hand, ε_G for C_D = 2 or 4 wt% in green compacts in the region of $p_C <$ 800 MPa. High isostatic pressure permitted the complete collapse of intergranular pores. Because intergranular pores have a negative effect on the densification of green compacts during sintering and on the bending strength distributions of the sintered bodies,[8] intergranular pores must collapse completely to produce highly reliable, high-strength ceramics. The granule strength must be designed to be as low as possible.

Because of the pseudobrittle fracture of spray-dried granules (Fig. 7), the mean diameter of the granules (d_G) in green compacts decreased during isostatic pressing, and the mean force

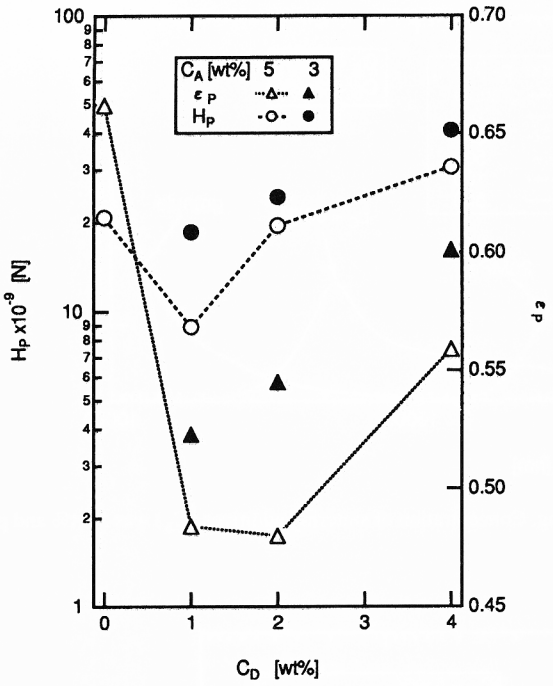

Fig. 12. Estimated porosity ratio of spray-dried granules (ε_P) and adhesion force (H_P) at contact point between primary Si_3N_4 particles.

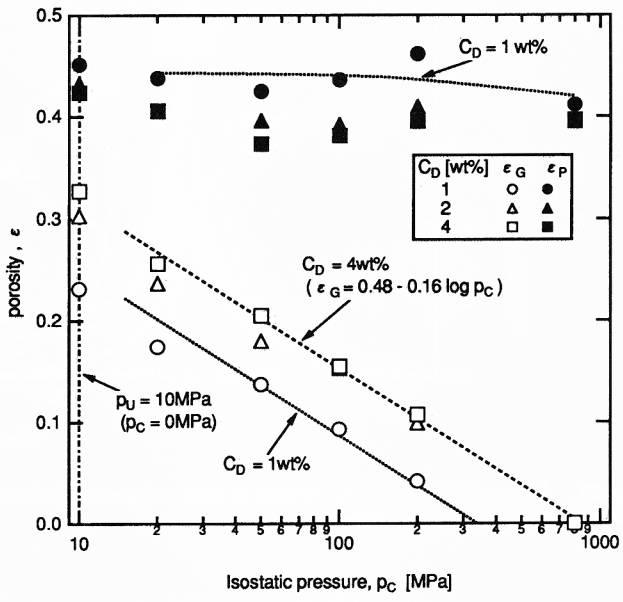

Fig. 14. Relations between intergranular (ε_G) and intragranular porosity ratio (ε_P) and isostatic pressure. Concentration of sintering additives (C_A) was 5 wt%.

(P) at the contact points between granules was related to the isostatic pressure according to the equation[27]

$$P = p_C d_G^2 \varepsilon_G/(1 - \varepsilon_G) \tag{10}$$

The contact force decreased with the decreasing mean diameter of the granules, and the value was related to the strength of the granules by the equation

$$P = K\pi d_G^2 \sigma_T \tag{11}$$

In the case of diametral compression between plates, the constant value of K was 1/2.8 (=0.357), which was used in Eq. (2). The value of K was, however, assumed to be larger than 0.357 and the complex function of d_G, ε_G, and other parameters, because the granules in the compact were pressed under different conditions. Substituting Eq. (11) into Eq. (10), and rearranging, gives the relationship between the intergranular porosity rate and the strength of the granules, σ_T, according to the following equation and Fig. 15.

$$\varepsilon_G/(1 - \varepsilon_G) = K\pi(\sigma_T/p_C) \tag{12}$$

The relationship between $\varepsilon_G/(1 - \varepsilon_G)$ and (σ_T/p_C) can be represented by

$$\varepsilon_G/(1 - \varepsilon_G) = 0.57\pi(\sigma_T/p_C)^{1/2} \tag{13}$$

The slope decreases to 1/2. In the region of $\sigma_T/p_C < 0.05$, in which range pressure is relatively high or granular strength low, and for which only one data point existed in the present study, the slope tends to increase to 1. Since high-strength granules cannot be collapsed at a relatively low isostatic pressure, the granules rearrange in the compacts. The slope in Fig. 15 thus decreased through the rearrangement of granules. At high isostatic pressure, because the rearrangement of granules in the compacts is complete and the main densification mechanism was collapse of the granules, Eq. (12) will be satisfied. If the granular strength is measured, this equation can determine the isostatic pressure that will completely collapse the intergranular porosity in green compacts.

The excessive amount of finely dispersed agglomerates in suspension caused increased fracture strength in the spray-dried granules and presented a wide range of large intergranular pores

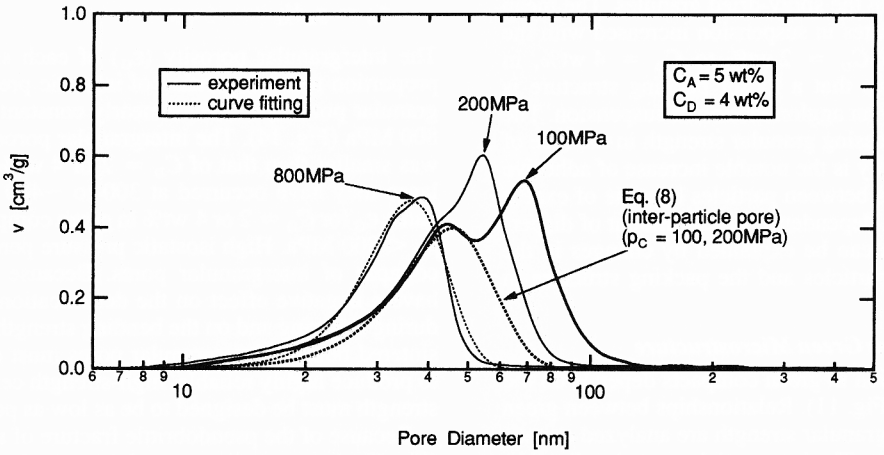

Fig. 13. Examples of analysis for pore size distribution in compacts.

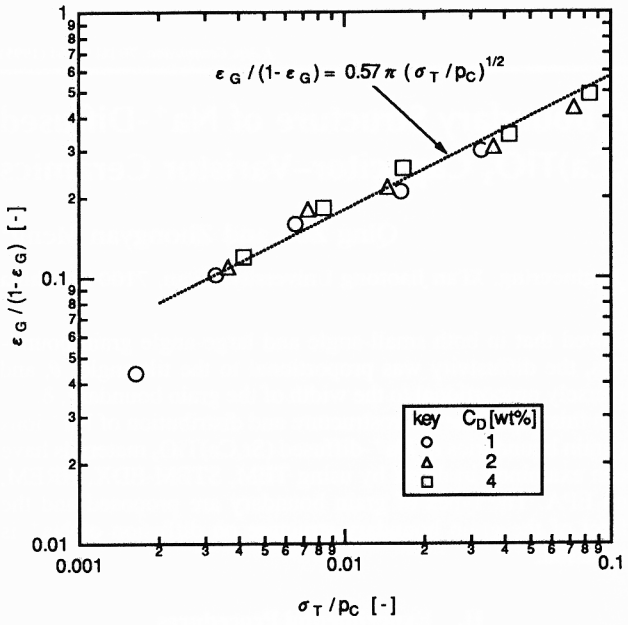

Fig. 15. Relations between intergranular porosity and the ratio of tensile strength of granules to isostatic pressure.

in the green compacts. The fracture strength of the spray-dried granules must be kept as low as possible, and the dispersion of agglomerates in suspension carefully controlled, to achieve uniform green compacts of Si_3N_4 powders with small and narrow pores.

V. Conclusions

The size of agglomerates in Si_3N_4 powders with 3 or 5 wt% of Al_2O_3 and Y_2O_3 ultrafine powders used as sintering aids was controlled by adding various amounts of a water-soluble polymeric dispersant. The effect of agglomerates in suspension on the microstructure of spray-dried granules and green compacts after isostatic pressing was discussed in this paper. The following conclusions can be made from the present results.

(1) An optimum concentration (C_D) of dispersant for obtaining a fine dispersion of agglomerates in suspension does exist. In the case of the maleic anhydride polymer used in this study, the optimum concentration was about 2 wt% with 5 wt% of sintering aids and 1 wt% with 3 wt% of sintering aids. Closely packed granules were prepared from the suspensions with finely dispersed agglomerates.

(2) The fracture strength of a single granule was measured directly by diametral compression testing. The fracture strength of each closely packed granule increased notably. The mechanisms for increasing granular strength include both the closely packed structure of the granules caused by the fine dispersion of agglomerates in suspension and the increased adhesive force at the contact points caused by excess dispersant.

(3) Even at the relatively high isostatic pressure (p_C = 200 MPa) used in the present study, intergranular pores present between unfractured granules in the green compacts had a negative effect on the densification of the sintered bodies. The intergranular pore volume and size increased with increasing fracture strength of the granules. Closely packed and high-strength granules required an isostatic pressure of 800 MPa to completely collapse and deform the intergranular pores.

(4) The isostatic pressure necessary to completely collapse the intergranular pores in green compacts could be estimated by Eq. (13). The strength of spray-dried granules must be as low as possible to obtain uniform green compacts of Si_3N_4 powders with small and narrow pores.

References

[1]R. A. Dimilia and J. S. Reed, "Dependence of Compaction on the Glass Transition Temperature of the Binder Phase," *Am. Ceram. Soc. Bull.*, **62** [4] 484–88 (1983).

[2]J. A. Brewer, R. H. Moore, and J. S. Reed, "Effect of Relative Humidity on the Compaction of Barium Titanate and Manganese Zinc Ferrite Agglomerates Containing Polyvinyl Alcohol," *Am. Ceram. Soc. Bull.*, **60** [2] 212–20 (1981).

[3]G. L. Messing, C. J. Markhoff, and L. G. McCoy, "Characterization of Ceramic Powder Compaction," *Am. Ceram. Soc. Bull.*, **61** [8] 857–60 (1982).

[4]J. Zheng and J. S. Reed, "Particle and Granule Parameters Affecting Compaction Efficiency in Dry Pressing," *J. Am. Ceram. Soc.*, **71** [11] C-456–C-458 (1988).

[5]R. L. K. Matsumoto, "Analysis of Powder Compaction Using a Compaction Rate Diagram," *J. Am. Ceram. Soc.*, **73** [2] 465–68 (1990).

[6]A. L. Salamone and J. S. Reed, "Preparation and Microscopic Analysis of Cellulose Binder Solutions," *Am. Ceram. Soc. Bull.*, **58** [6] 618–19 (1979).

[7]S. J. Lukasiewicz, "Spray-Drying Ceramic Powders," *J. Am. Ceram. Soc.*, **72** [4] 617–24 (1989).

[8]A. Roosen and H. K. Bowen, "Influence of Various Consolidation Techniques on the Green Microstructure and Sintering Behavior of Alumina Powders," *J. Am. Ceram. Soc.*, **71** [11] 970–77 (1988).

[9]M. Kumagai and G. L. Messing, "Controlled Transformation and Sintering of a Boehmite Sol–Gel by α-Alumina Seeding," *J. Am. Ceram. Soc.*, **68** [9] 500–509 (1985).

[10]M. D. Sacks and T. Y. Tseng, "Preparation of SiO_2 Glass from Model Powder Compact: I, Formation and Characterization of Powders, Suspensions, and Green Compacts," *J. Am. Ceram. Soc.*, **67** [8] 526–32 (1984).

[11]M. D. Sacks and T. Y. Tseng, "Preparation of SiO_2 Glass from Model Powder Compact: II, Sintering," *J. Am. Ceram. Soc.*, **67** [8] 532–37 (1984).

[12]T.-S. Yen and M. D. Sacks, "Low-Temperature Sintering of Aluminum Oxide," *J. Am. Ceram. Soc.*, **71** [10] 841–44 (1988).

[13]W. H. Rhodes, "Agglomerate and Particle Size Effects on Sintering Yttria-Stabilized Zirconia," *J. Am. Ceram. Soc.*, **64** [1] 19–22 (1981).

[14]A. V. Kerkar, R. J. M. Henderson, and D. L. Feke, "Steric Stabilization of Nonaqueous Silicon Slips: I, Control of Particle Agglomeration and Packing," *J. Am. Ceram. Soc.*, **73** [10] 2879–85 (1990).

[15]A. V. Kerkar, R. J. M. Henderson, and D. L. Feke, "Steric Stabilization of Nonaqueous Silicon Slips: II, Pressure Casting of Powder Compacts," *J. Am. Ceram. Soc.*, **73** [10] 2886–91 (1990).

[16]H. Hsieh and T. Fang, "Effect of Green States on Sintering Behavior and Microstructural Evolution of High-Purity Barium Titanate," *J. Am. Ceram. Soc.*, **73** [6] 1566–73 (1990).

[17]S. Sumita, W. E. Rhine, and H. K. Bowen, "Effects of Organic Dispersants on the Dispersion, Packing, and Sintering of Alumina," *J. Am. Ceram. Soc.*, **74** [9] 2189–96 (1991).

[18]H.-W. Lee and M. D. Sacks, "Pressureless Sintering of SiC-Whisker-Reinforced Al_2O_3 Composites: I, Effect of Matrix Powder Surface Area," *J. Am. Ceram. Soc.*, **73** [7] 1884–93 (1990).

[19]H.-W. Lee and M. D. Sacks, "Pressureless Sintering of SiC-Whisker-Reinforced Al_2O_3 Composites: II, Effects of Sintering Additives and Green Body Infiltration," *J. Am. Ceram. Soc.*, **73** [7] 1894–900 (1990).

[20]W. J. Tseng and P. D. Funkenbusch, "Microstructure and Densification of Pressureless-Sintered/SiN-Whisker Composites," *J. Am. Ceram. Soc.*, **75** [5] 1171–75 (1992).

[21]K. Uematsu, J.-Y. Kim, M. Miyashita, N. Uchida, and K. Saito, "Direct Observation of Internal Structure in Spray-Dried Alumina Granules," *J. Am. Ceram. Soc.*, **73** [8] 2555–57 (1990).

[22]K. Uematsu, M. Miyashita, J.-Y. Kim, and N. Uchida, "Effect of Forming Pressure on the Internal Structure of Alumina Green Bodies Examined with Immersion Liquid Technique," *J. Am. Ceram. Soc.*, **74** [9] 2170–74 (1991).

[23]P. K. Whitman and D. L. Feke, "Comparison of the Surface Charge Behavior of Commercial Silicon Nitride and Silicon Carbide Powders," *J. Am. Ceram. Soc.*, **71** [12] 1086–93 (1988).

[24]K. Honma, H. Okada, and T. Tateno, "Effects of Starting Powders on Properties of Normally Sintered and HIP'ed Si_3N_4," *J. Ceram. Soc. Jpn.*, **95** [3] 323–29 (1987).

[25]T. M. Shaw and B. A. Pethica, "Preparation and Sintering of Homogeneous Silicon Nitride Green Compacts," *J. Am. Ceram. Soc.*, **69** [2] 88–93 (1986).

[26]S. P. Timoshenko and J. N. Goodier, *Theory of Elasticity*, 3rd ed.; pp. 409–14. McGraw-Hill, New York, 1982.

[27]Y. Hiramatsu, Y. Oka, and H. Kiyama, "Determination of the Tensile Strength of Rock by a Compression Test of an Irregular Test Piece," *J. Min. Eng. Jpn.*, **81**, 1024–30 (1965).

[28]J. Y. Wong, S. E. Laurich-Mcintype, A. K. Khaund, and R. C. Bradt, "Strength of Green and Fired Spherical Aluminosilicate Aggregates," *J. Am. Ceram. Soc.*, **70** [10] 785–91 (1987).

[29]D. E. Niesz, R. B. Bennett, and M. J. Snyder, "Strength Characterization of Powder Aggregates," *Am. Ceram. Soc. Bull.*, **51** [9] 677–80 (1972).

[30]J. S. Reed, *Introduction to the Principles of Ceramics Processing*; pp. 338–45. Wiley, New York, 1987.

[31]H. Kamiya, H. Suzuki, D. Kato, and G. Jimbo, "Densification of Alkoxide-Derived Fine SiO_2 Powder Compact by Ultra-high Pressure Cold Isostatic Pressing," *J. Am. Ceram. Soc.*, **76** [1] 54–64 (1993).

[32]H. Kamiya, H. Suzuki, T. Ichikawa, and G. Jimbo, "Ultra-High Pressure Cold Isostatic Pressing–Low Temperature Sintering of Alkoxide-Derived Mullite Precursor Powders," *Ceram. Eng. Sci. Proc.*, **13** [7–8] 563–70 (1992).

[33]H. Rumpf, "Zur Theorie der Zugfestigkeit von Agglomeraten bei Kraftubertragung an Kontaktpunkten," *Chem.-Ing.-Tech.*, **42**, 538–40 (1970).

[34]J. Tsubaki and G. Jimbo, "Theoretical Analysis of the Tensile Strength of a Powder Bed," *Powder Technol.*, **37**, 219–27 (1984). □